



CHARACTERISATION OF HYBRID GRAPHENE NANOPLATELETS WITH FUNCTIONALISED BORON NITRIDE AS THERMAL INTERFACE MATERIAL



DOCTOR OF PHILOSOPHY

2023



Faculty of Mechanical Engineering



**CHARACTERISATION OF HYBRID GRAPHENE
NANOPLATELETS WITH FUNCTIONALISED BORON NITRIDE
ASTHERMAL INTERFACE MATERIAL**

Solehah Binti Jasmee

Doctor of Philosophy

2023

**CHARACTERISATION OF HYBRID GRAPHENE NANOPATELETS WITH
FUNCTIONALISED BORON NITRIDE AS THERMAL INTERFACE MATERIAL**

SOLEHAH BINTI JASMEE



UNIVERSITI TEKNIKAL MALAYSIA MELAKA

2023

DECLARATION

I declare that this thesis entitled “Characterisation of Hybrid Graphene Nanoplatelets with Functionalised Boron Nitride as Thermal Interface Material” is the result of my own research except as cited in the references. The thesis has not been accepted for any degree and is not concurrently submitted in candidature of any other degree.

Signature

: 

Name

: SOLEHAH BINTI JASMEE

Date

: 19/10/2023

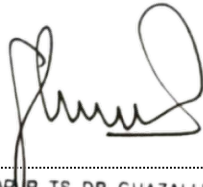
اونيورسيتي تيكنيكل مليسيا ملاك

UNIVERSITI TEKNIKAL MALAYSIA MELAKA

APPROVAL

I hereby declare that I have read this thesis and in my opinion, this thesis is sufficient in terms of scope and quality for the award of Doctor of Philosophy.

Signature :



Supervisor Name :

PROFESOR R. TS. DR. GHAZALI BIN OMAR
Timbalan Naib Canselor (Penyelidikan & Inovasi)
Universiti Teknikal Malaysia Melaka

Date :

19/10/2023



اونيورسيتي تيكنيكل مليسيا ملاك

UNIVERSITI TEKNIKAL MALAYSIA MELAKA

DEDICATION

To my beloved mother, father, siblings and my best friend.



ABSTRACT

Conductive fillers with a polymer matrix or Thermal Conductive Adhesive (TCA) have met most of the ideal criteria due to being ecologically friendly, reliable, and affordable. However, this effort may not yet lead to a significant technology breakthrough due to the low thermal conductivity of the polymer and the high filler loading used in a single-filled composite. Hence, it has heightened the need for hybrid fillers with extraordinary properties, such as boron nitride (BN) and graphene nanoplatelets (GNPs), at varying sizes with the incorporation of silane-modified BN (fBN) to improve composite's properties. Yet, the affirmative review shows very few studies have reported on the hybrid composite GNPs with fBN at different filler sizes and lower filler loading (<20 wt.%), as well as its suitable processing parameter and important characterization such as rheological, water absorption, and adhesion strength with and without moisture. Thus, this study seeks to determine the curing time, temperature, and mixing method of the composite, percolation threshold of thermal conductivity of single composite GNPs, BN, and fBN, and thermal conductivity of hybridized GNPs with BN or fBN below filler loading of single composite and also to characterize the rheological properties, adhesion strength (single lap joint (SLJ) approach) and failure mechanism of hybridized GNPs with BN or fBN composite at ambient and 100% humidity conditions. The hybrid composites were prepared by hybridizing different ratios of GNPs (5 μm and 15 μm) with BN or fBN (10 μm) that were modified using silane coupling agents (KH550 and KH560). KD2 Pro and Anton Paar Rheometer MCR 72 were used to measure thermal conductivity and rheological properties, while the SLJ test was prepared and accordance with ASTM D1002, ASTM D 1151, ASTM D 5229/D 5229M, and EN ISO 10365 standards. The result indicates that hybrid GNPs15/fBN_KH560 composites exhibit the highest thermal conductivity (1.16 ± 0.02 W/mK) at a GNPs15 ratio 0.75. However, hybrid GNP5 composites have a higher shear strength than hybrid GNP15 composites at all GNPs ratios, with the highest values reported being 1.20 ± 0.10 MPa and 1.14 ± 0.15 MPa at GNPs ratio of 0.75 with fBN_KH560. The bigger filler size of GNPs may help to transfer heat, but smaller fillers are preferable to transfer stress. The failure mechanisms like plastic void growth, crack deflection, particle debonding, and pull-out mechanism also help promote cohesive failure in the hybrid composite. Hybrid GNP15 composites have high shear strength and absorb more water than hybrid GNP5 but can sustain for 30 days before reaching equilibrium. The larger filler particle fills the gaps between the epoxy, reducing the formation of cracks or voids. Nevertheless, moisture still caused the shear strength of composites to reduce (0.39 ± 0.05 MPa). In summary, the properties of hybrid composites containing fBN_KH560, especially at GNPs ratio of 0.75, show outstanding properties due to high compatibility between fBN_KH560 and the polymer matrix, proven by the lowest measured contact angle, and Hansen solubility parameter difference, well-dispersed filler, and better wetting properties (lowest viscosities varies shear rate) in rheological analysis.

PENCIRIAN HIBRID GRAFEN NANOPLETETS BERFUNGSIKAN BORON NITRIDA SEBAGAI BAHAN ANTARA MUKA TERMA

ABSTRAK

Pengisi konduktif dengan matriks polimer atau Pelekat Konduktif Terma (TCA) telah memenuhi kebanyakan kriteria ideal seperti mesra alam, boleh dipercayai dan berpatutan. Namun, usaha ini belum mampu membawa kepada kejayaan teknologi yang ketara disebabkan oleh kekonduksian haba polimer yang masih rendah dan pemuatan pengisi yang tinggi dalam sesuatu komposit. Oleh itu, ia telah meningkatkan keperluan untuk menghibrid pengisi yang mempunyai sifat yang luar biasa seperti boron nitrida (BN) dan grafen nanoplatelets (GNPs), pada saiz yang berbeza dan dengan penggabungan BN yang diubahsuai (fBN) dengan silane untuk meningkatkan ciri-ciri komposit. Namun, semakan afirmatif menunjukkan sangat sedikit kajian melaporkan tentang GNP komposit hibrid dengan fBN pada saiz pengisi yang berbeza dan pemuatan pengisi yang rendah (<20 berat.%), serta parameter pemprosesan yang sesuai dan pencirian penting seperti reologi, penyerapan air, dan kekuatan lekatan dengan dan tanpa kelembapan. Justeru, kajian ini dijalankan untuk menentukan tempoh pengesetan, suhu pengesetan, dan kaedah campuran komposit yang sesuai, ambang perkolasi keberkonduktan terma bagi komposit tunggal GNPs, BN, dan fBN juga apabila dihibridkan dibawah pengisi pemuatan komposit tunggal dan juga untuk mencirikan sifat reologi, kekuatan lekatan (pendekatan ujian sendi tunggal (SLJ)) dan mekanisme kegagalan hibrid GNPs dengan BN atau fBN pada suhu sekeliling dan 100% kelembapan. Komposit hibrid disediakan dengan mengacukan berbeza nisbah antara GNPs (5 μ m dan 15 μ m) dengan BN atau fBN (10 μ m) yang diubah suai dengan ejen gandingan silane (KH550 dan KH560). KD2 PRO dan Anton Paar Rheometer MCR 72 digunakan untuk mengukur kekonduksian terma dan sifat reologi manakala SLJ disediakan berdasarkan ASTM D1002 ASTM D 1151, ASTM D 5229/D 5229M dan EN ISO 10365. Hasilnya menunjukkan bahawa hibrid komposit GNPs15/fBN_KH560 mempamerkan kekonduksian terma tertinggi (1.16 \pm 0.02 W/mK) pada nisbah GNPs15 0.75. Namun, alisis kekuatan ricih menunjukkan hibrid komposit GNPs5 lebih tinggi berbanding hibrid komposit GNPs15 pada semua nisbah GNPs dengan nilai tertinggi adalah 1.20 \pm 0.10 MPa dan 1.14 \pm 0.15 MPa pada GNPs ratio of 0.75 dengan fBN_KH560. Saiz pengisi GNP yang lebih besar membantu memindahkan haba, tetapi pengisi yang lebih kecil adalah lebih baik untuk memindahkan tekanan. Mekanisme kegagalan seperti pertumbuhan lompong plastik, pesongan retak, penyahikatan zarah, dan mekanisme tarik keluar juga membantu menggalakkan kegagalan kohesi dalam komposit hibrid. Walau bagaimanapun, komposit GNP15 hibrid dilihat menyerap lebih banyak air daripada GNP5 hibrid tetapi mampu bertahan sehingga 30 hari sebelum mencapai keseimbangan. Pengisi yang lebih besar mengisi jurang antara epoksi, mengurangkan pembentukan retakan atau lompong. Namun, lembapan masih menyebabkan kekuatan ricih komposit berkurangan (0.39 \pm 0.05 MPa). Ringkasnya, komposit hibrid yang mengandungi fBN terutamanya pada nisbah GNPs 0.75 menunjukkan ciri yang menonjol kerana keserasian yang tinggi antara fBN_KH560 dan matriks polimer, dibuktikan oleh sudut sentuhan terukur dan perbezaan parameter keterlarutan Hansen yang rendah, pengisi tersebar dengan baik, dan sifat pembasahan yang lebih baik (kelikatan terendah pada kadar ricih berbeza) dalam analisis reologi.

ACKNOWLEDGEMENTS

In the Name of Allah, the Most Gracious, the Most Merciful

First and foremost, I would like to thank and praise Allah the Almighty, my Creator, my Sustainer, for everything I have received since the beginning of my life. I want to extend my appreciation to the Universiti Teknikal Malaysia Melaka (UTeM) for providing the research platform, and the Malaysian Ministry of Higher Education (MOHE) for the financial support throughout this project (FRGS/2018/FKM-CARe/ F00366). Sincere gratitude to my main supervisor, Prof. Ir Ts. Dr. Ghazali bin Omar for his guidance, kindness and encouragement throughout my study. May Allah give you the ultimate happiness you want in your life.

My deepest gratitude to my parents, Jasmee bin Zali and A'fifah binti Mohamed, and my siblings for their endless support, love, prayers, and faith in me. My utmost appreciation goes to my beloved one, Siti Syahirah binti Che Othaman, who has been the pillar of strength in all my endeavours. This journey is impossible without you. Not to forget my fellow postgraduate colleagues and my lectures in the Advance Materials Characteristic Laboratory (AMCHAL) (PM Dr. Siti Hajar Sheikh Md Fadzullah, Dr. Nadlene Razali and Dr. Mizah Ramli) for their support, courage, knowledge, and invaluable help. My sincere appreciation also extends to my dear friends (Atul, Lily, Aziera, and Biha) for always looking up to me. Thank you, Jemahs. Also, thanks to the assistance engineers in the Faculty of Mechanical Engineering for the assistance and support I received during the research work, especially for En Mahader. Finally, thank you to everyone who had been to the crucial parts of the realisation of this study. My humble apology, as it is beyond my reach, not to mention those involved directly or indirectly. Thank you.

TABLE OF CONTENTS

	PAGE
DECLARATION	
APPROVAL	
DEDICATION	
ABSTRACT	i
ABSTRAK	ii
ACKNOWLEDGEMENTS	iii
TABLE OF CONTENTS	iv
LIST OF TABLES	vii
LIST OF FIGURES	ix
LIST OF ABBREVIATIONS	xvii
LIST OF SYMBOLS	xix
LIST OF PUBLICATIONS	xx
CHAPTER 1 INTRODUCTION	1
1.1 Background	1
1.2 Problem statement	10
1.3 Research objective	12
1.4 Scope of study	13
1.5 Hypothesis/ research questions	14
1.6 Thesis outline	15
CHAPTER 2 LITERATURE REVIEW	17
2.1 Overview	17
2.2 Thermal management	17
2.2.1 Thermal interface material	22
2.2.2 Interface thermal resistance / Kapitza resistance	39
2.2.3 Factor affecting interface thermal resistance	43
2.3 Recent studies of TCA	55
2.3.1 Single filler polymer composite	56
2.3.2 Hybrid polymer composite	64
2.3.3 Reliability of TCA as an epoxy-based composite	81
2.3.4 Failure mode and failure mechanism of polymer composite	82
2.4 Surface treatment of conductive fillers	94
2.5 Contact angle and Hensen solubility parameter	101

2.6	Consideration parameter for polymer composite preparation	104
2.6.1	Stoichiometric ratio	104
2.6.2	Curing reaction	105
2.6.3	Method of mixing	107
2.7	Research gap	112
CHAPTER 3 METHODOLOGY		114
3.1	Overview	114
3.2	Flowchart	114
3.3	Materials	118
3.3.1	Graphene nanoplatelets	118
3.3.2	Boron nitride	119
3.3.3	Araldite® M	120
3.3.4	Jeffamine D230	121
3.3.5	Silane coupling agent	122
3.3.6	Ethanol	123
3.4	Parametric study of TCA composite	123
3.4.1	Stoichiometric ratio	124
3.4.2	Determination of curing temperature via Differential Scanning Calorimetry	124
3.4.3	Determination of curing time and cross-link level via Vickers Hardness analysis	126
3.4.4	Determination of mixing method	128
3.5	Surface modification of BN	129
3.6	Preparation of single and hybrid composite	130
3.7	Sample preparation	134
3.7.1	Sample preparation for thermal conductivity characterisation	134
3.7.2	Sample preparation for moisture absorption and lap shear characterisation	135
3.8	Characterisation	138
3.8.1	Chemical analysis	138
3.8.2	Thermal conductivity analysis	140
3.8.3	Contact angle measurement	141
3.8.4	Hansen solubility parameter	142
3.8.5	Rheological analysis	143
3.8.6	Moisture absorption analysis	143
3.8.7	Mechanical properties analysis of lap shear strength using single lap joint (SLJ) approach	145
3.8.8	Microstructure analysis	147
3.9	Summary	149
CHAPTER 4 RESULTS AND DISCUSSION		150
4.1	Introduction	150
4.2	Parametric results of thermally conductive adhesive polymer composite	150
4.2.1	Thermal analysis for curing temperature of composite via Differential Scanning Calorimetry	150
4.2.2	Cross-linking level and curing time via Vickers Hardness analysis	152

4.2.3	Distribution and dispersion of GNPs filler in the polymer matrix at different mixing methods	156
4.2.4	Summary	164
4.3	Characterisation of fillers	165
4.3.1	Chemical analysis of boron nitride functionalised silane	165
4.3.2	Analysis of contact angle and Hensen Solubility Parameter (HSP) of functionalized BN	167
4.3.3	Chemical analysis of pristine GNPs using Raman Spectroscopic	169
4.4	Thermal conductivity analysis	173
4.4.1	Percolation threshold of a single composite	174
4.4.2	Thermal conductivity of hybrid composite	184
4.5	Analysis of rheological properties of single and hybrid GNPs/BN composite	194
4.5.1	Rheological properties of single composite GNPs, BN and fBN composite	195
4.5.2	Rheological properties of Hybrid GNPs/BN and GNPs/fBN	204
4.6	Moisture content analysis	209
4.7	Mechanical properties analysis of single and hybrid GNPs/BN composite	215
4.7.1	Lap shear strength analysis of hybrid composite	216
4.7.2	Effect of moisture on lap shear strength	228
CHAPTER 5	CONCLUSION AND RECOMMENDATIONS	235
5.1	Conclusion	235
5.2	Contribution to research work	237
5.3	Recommendations	238
REFERENCES		240

LIST OF TABLES

TABLE	TITLE	PAGE
2.1	Summary of the types of existing TIMs and their advantages and disadvantages	35
2.2	Intrinsic thermal conductivity properties for each type of filler	44
2.3	Properties of GNPs used respected to defect density and thermal conductivity (Shtein et al., 2015a)	49
2.4	Properties of nanosized Al ₂ O ₃ particles (Reprint with permission (Xie et al., 2002))	51
2.5	Summary of single filler used in polymer composite for different types, filler sizes, and shapes	62
2.6	Summary of hybrid polymer composite	77
2.7	Limitation characterisation of hybrid GNPs and BN	79
2.8	Summary of surface treatment used from literature studies	97
2.9	Example of <i>Fdi</i> , <i>Fpi</i> , <i>Fhi</i> , and <i>Vm</i> of functional groups based on Fedor's method (Gadade et al., 2017; Jankovic et al., 2019)	104
2.10	Summary of the mixing method	111
3.1	Properties of GNPs 5 μm and 15 μm	119
3.2	Properties of BN fillers	120
3.3	Properties of Araldite® M	121
3.4	Properties of curing agent Jeffamine D230	122
3.5	Properties of silane coupling agents KH-550 and KH-560	123
3.6	Description of samples for DSC testing	123

3.7	Composition of polymer composite at different epoxy resin and curing agent ratios	129
3.8	Composition of single-filled composite GNP _s 5, GNP _s 15, BN and fBN	131
3.9	Composition for hybrid GNP _s 5-filled composites at a total filler loading of 15 %	132
3.10	Composition for hybrid GNP _s 15-filled composites at a total filler loading of 12 %	132
4.1	Thermal conductivity of GNP _s 5 composite at different mixing methods and ratios	164
4.2	Optimisation of processing parameter of TCA polymer composite	165
4.3	Calculated Solubility parameters of epoxy resin, KH550, and KH560 of the study	169
4.4	Intensity of defect density (I_D/I_G) and doping level (I_{2D}/I_G) of GNP _s 5 and GNP _s 15	173
4.5	Yield stress value of single-filled composite GNP _s 5, GNP _s 15, BN, fBN_KH550 and fBN_KH560	201
4.6	Yield stress value (Pa) of hybrid composite GNP _s 5 and GNP _s 15 with BN, fBN_KH550 and fBN_KH560	207
4.7	Failure analysis for hybrid GNP _s 5 composites at different GNP _s 5 ratios	221
4.8	Failure analysis for hybrid GNP _s 15 composites at different GNP _s 15 ratios	226
4.9	Failure analysis for hybrid GNP _s 5 with BN and fBN composite at different GNP _s 5 ratios after exposure to moisture	231
4.10	Failure analysis for hybrid GNP _s 15 with BN and fBN composite at different GNP _s 15 ratios after exposure to moisture	232

LIST OF FIGURES

FIGURE	TITLE	PAGE
2.1	Identical CPU boards using a heatsink (left) and heat spreader (right)	20
2.2	Schematic diagram of roughness and waviness present between two contacting surfaces	23
2.3	Schematic of power package device for (a) high thermal dissipation package device, (b) low thermal dissipation package device, (c) real power packaging devices (Schmidt, 2020)	24
2.4	Schematic diagram of TIM inserted between the two contacting materials	27
2.5	(a) Flow curves, (b) viscosity curves for (1) ideally viscous, (2) shear-thinning, and (3) shear-thickening flow behaviour (Anton Paar, 2023)	29
2.6	Consideration factor selecting TIM	31
2.7	Mechanism of the thermal percolation threshold	38
2.8	Illustration of TCR and TBR when mixing the fillers and polymer matrix	40
2.9	Schematic illustration of heat transfer mechanism through phonon spectra (Li et al., 2017a)	41
2.10	Factors needed to be considered in order to design new materials for high thermal conductivity (Chen et al., 2016)	42
2.11	Interfacial area of (a) small and (b) large filler sizes	45
2.12	Thermal conductivity of polymer composite at different filler sizes of BN and volume fraction of filler (Zhou et al., 2007)	46

2.13	Thermal conductivity increase as the BN filler size increase (Pawelski et al., 2019)	47
2.14	(a) thermal conductivity of BN at different filler sizes (2 μm , 30 μm and 180 μm), Scanning electron morphology of contact area of filler (b) 2 μm (c) 30 μm (d) 180 μm (Moradi et al., 2019)	48
2.15	Contact area at different sizes: (a) large filler and (b) small filler	48
2.16	Direction of heat transfer: (a) longitudinal (in-plane) and (b) perpendicular (through-plane)	52
2.17	Shape of (a) 0D (nanoparticles), (b) 1D (fibre, rods, tubes, wires), (c) 2D (platelets, sheets, flakes) fillers, (d–e) agglomeration, (f) stacking of each nanofiller	54
2.18	(a) Smooth-shaped and (b) irregular-shaped fillers	55
2.19	Enhancement of thermal conductivity for different shapes of SiC fillers (Liu et al., 2017)	58
2.20	Schematic of the atomic arrangement in graphene layer coupling (Pop et al., 2012)	60
2.21	(a) thermal conductivity of pristine Ag epoxy, hybrid graphene/Ag epoxy composite and graphene/CB epoxy composite (b) morphology of hybrid graphene/Ag epoxy composite (Goyal and Balandin, 2012)	65
2.22	Heat conduction path/ network of (a) single filler and (b) hybrid fillers with different sizes	67
2.23	(a) Thermal conductivity of pristine BN, M 15, and hybrid at different volume fractions; (Hybrid1_M15:0.15, BN:0.02; Hybrid2_M15:0.17, BN:0.03) and, schematic (b) optimal amount of hybridising GNPs/BN (c) Excessive BN filler loading (Shtein et al., 2015b)	68

2.24	SEM image of (a) gaps between metal copper filler (b) Aggregation of GNPs C-500 filled the gaps (c) Few GNPs H-15 filled the gaps (d) thermal conductivity of hybrid composite metal-GNP (C-500 and H-15) hybrid composite (Rad et al., 2019)	70
2.25	Schematic diagram of the 3D network formed when hybridising: (a) 2D with 0D, (b) 2D with 1D, (c) 1D with 0D, (d) contact area, (e) point-contact, (f) face-contact (g) point-contact	71
2.26	Intercalating of CU fillers as a spacer in between graphene filler (a) Schematic(b) SEM image (Barani et al., 2019)	72
2.27	Microstructure of (a) CNTs absorbed on the GNPs surface; (b)–(d) Bridges formed between CNTs and GNPs (Wang et al., 2020a)	73
2.28	(a) SEM Image of BNNS/BNNT in the epoxy matrix (b) Schematic illustration of BNNT/BNNS network (c) thermal conductivity of BNNT/Epoxy, BNNS/Epoxy and BNNS/BNNT/Epoxy (Su et al., 2013)	74
2.29	Illustration of (a) crack growth in nonreinforced bond line, (b) crack growth deviation after fillers reinforced, (c) AF mode, (d) CF modes, (e) crack growth deviation subjected to partial fatigue loading, (f) and (g) mixed AF and CF mode (NajiMehr et al., 2022)	84
2.30	SEM images of the fractured surfaces for the MWCNT composite, (a) schematic of reinforcing mechanisms, (b) pull-out, crack arrest and crack deviation path, (c) pull-out, (d) pull-out in the change of crack growth plane, (e) and (f) crack bridging of MWCNT (NajiMehr et al., 2022)	86
2.31	SEM images of the fractured surfaces for the GNP composite, (a) schematic of reinforcing mechanism s, (b) breakage of GNP and crack arrest, (c) partial pull-out and particle deformation, (d) deviation of crack growth path (NajiMehr et al., 2022)	87

2.32	Fracture surfaces and failure mode of (a) unreinforced polymer, (b) Single composite of 0.5 wt.% MWCNTs, (c) Single composite of 0.8 wt.% SNPs, (d) Hybrid composite (Epoxy + 0.4 wt.% MWCNTs + 0.4 wt.% SNPs) (Razavi et al., 2018)	88
2.33	Failure mechanism of the (a) pull-out mechanism of nanotubes, (b) micro crack growth deviation in the adhesive layer reinforced with MWCNTs, (c) Particles debonding with subsequent plastic void growth at 0.8 wt.% of silica nanoparticles (Razavi et al., 2018)	89
2.34	Schematic illustration and SEM micrographs of different mechanisms activated by the hybrid incorporation of GNPs and SNPs in the polymer matrix (Zamani et al., 2022)	91
2.35	SEM images of aged epoxy composites (a) undoped (b) hBN doped	93
2.36	Dependence of the surface wettability on the contact angle, θ	101
2.37	Research gap of study	113
3.1	Flowchart of research work	117
3.2	SEM image of (a) GNPs 5 μm (b) GNPs 15 μm (c) GNPs filler	119
3.3	(a) Purchased BN filler, (b) SEM image of BN filler	120
3.4	Epoxy resin Araldite	121
3.5	Jeffamine D230	122
3.6	(a) TA Instruments Q20 Differential Scanning Calorimetry; (b) Hermetic Al sample pan	125
3.7	Mixture of epoxy resin and curing agent mixture (a) not fully opaque (b) opaque	126

3.8	(a) Representative sample set-up using Shimadzu Micro Hardness Tester HMV-G21 (b) The indentation of Vickers indenter	127
3.9	(a) GT bath sonication (b) Planetary Centrifugal Thinky Mixer Model ARE-310 (c) LABSONIC® P Ultrasonic Homogenizer	128
3.10	Schematic illustration of the surface modification of BN	130
3.11	Step-by-step preparation of polymer composite	133
3.12	(a) Samples in a silicone mould (b) representative of cured sample	134
3.13	SLJ specimen with dimension (a) top view (b) side view (c) actual representative sample	135
3.14	(a) Real jig fixture as SLJ specimen's holder (b) Schematic of jig fixture with dimension (c) Side view of a schematic of jig fixture with SLJ specimen	137
3.15	UniRAM-3500 Raman spectroscopy	139
3.16	Thermo Nicolet iS10 Attenuated Total Reflection (ATR)- Fourier 138Transform Infrared Spectroscopy (FTIR)	140
3.17	(a) KD2 Pro Thermal Analyzer, (b) schematic diagram of thermal conductivity measurement	141
3.18	Schematic diagram of self-fabricated contact angle tool	142
3.19	Anton Paar Rheometer MCR 72 Equipment	143
3.20	Immersed sample in the (a) aluminium container, (b) oven for moisture absorption analysis	145
3.21	Instron 8872 UTM	146
3.22	Setup of lap shear testing on a universal testing machine	147

3.23	(a) Scanning Electron Microscope (Model JSM-6010PLUS/LV, Jeol Ltd.), (b) Nano 2000T Grinder-Polisher, (c) Auto fine coater Model JEOL JEC-3000FC (USA)	148
3.24	Sample of (a) Cross-section for filler dispersion characterisation and (b) fractured sample after the SLJ test	149
4.1	DSC curve of epoxy resin and curing agent at the pure condition and different epoxy resin/ curing agent ratio	152
4.2	(a) uncured mixture of 1:1 ratio; indentation marks of 2:1 ratio after (b) 1 second (c) 3 second	153
4.3	Chemical structure of (a) epoxy resin 506 (b) Curing agent Jeffamine D-230 (c) Cross-linked epoxy resin and curing agents	155
4.4	Vickers hardness and indentation marks for ratio 3:1	156
4.5	Surface morphology of the GNPs composite using Planetary Centrifugal Thinky Mixer at the ratio of (a) 2:1 (x700), (b) 2:1 (x2000), (c) 3:1 (x700), (d) 3:1 (x2000)	158
4.6	Surface morphology of the GNPs composite using an ultrasonic homogeniser at the ratio of (a) 2:1 (x700), (b) 2:1 (x2000), (c) 3:1 (x700), (d) 3:1 (x2000)	161
4.7	Illustration of distribution and dispersion of GNPs fillers at the ratio (a)(b) 2:1, (c)(d) 3:1	162
4.8	FTIR spectra of pristine BN, fBN_KH550, and fBN_KH560	167
4.9	Contact angle of polymer matrix on (a) BN (b) fBN_KH550 (c) fBN_KH 560	168
4.10	Raman spectra of pristine GNP5 and GNP15 at (a) D Peak and G peak and (b) 2D peak	173

4.11	Thermal conductivity of single-filled composites (a) GNPs5 and GNPs15, (b) BN and fBN (KH550 and KH560)	176
4.12	SEM cross-sectional morphology of single filled composite of (a) GNPs5 at 5 wt.% (b) GNPs5 at 15 wt.%; (c) GNPs15 at 12 wt.% (d) GNPs15 at 15 wt.%	178
4.13	Chemical reaction of (a) fBN_KH550 with epoxy resin and (b) fBN_KH560 with curing agent (c) chemical structure of the compound in epoxy resin and curing agent	180
4.14	SEM cross-sectional image of single filled BN composite at filler loading of (a) 20 wt.% (b) 40 wt.%	182
4.15	SEM cross-sectional image of single filled fBN_KH550 composite filler loading of (a) 20 wt.% (b) 40 wt.%	183
4.16	SEM cross-sectional image of single filled fBN_KH560 filler loading of (a) 20 wt.% (b) 40 wt.%	184
4.17	Thermal conductivity of hybrid composites GNPs5/BN and GNPs5/fBN at different GNPs ratio	185
4.18	SEM cross-sectional image of the hybrid composite at GNPs ratio of 0.75 (a) GNPs5/BN (b) GNPs5/fBN_KH550 (c) GNPs5/fBN_KH560	187
4.19	Distribution of filler at GNPs5 ratio of (a) 1.00 (b) 0.75	189
4.20	Thermal conductivity of hybrid composites GNPs15/BN and GNPs15/fBN at different filler ratio	191
4.21	SEM cross-sectional image of hybrid composite at GNPs15 ratio of 0.75 (a) GNPs15/BN (b) GNPs15/fBN_KH550; (c) GNPs15/fBN_KH560	193
4.22	Viscosity vs shear rate of single-filled composite (a) GNPs5 and GNPs15 (b) BN and fBN	198

4.23	The flow curves of single-filled composite (c) GNPs5 and GNPs15 (d) BN and fBN	200
4.24	Plot G' , G'' versus angular frequency of single-filled composite (a) GNPs5, (b) GNPs15 and (c) BN and fBN	204
4.25	(a) Viscosity vs shear rate (b) flow curve plot; of hybrid composite GNPs5 and GNPs15 with BN and fBN at GNPs ratios f 0.75	207
4.26	Plot G' , G'' vs angular frequency of hybrid composite (a), GNPs5, (b) GNPs15; with BN and fBN	209
4.27	Moisture content of (a) GNPs5/BN, (b) GNPs5/fBN_KH550, (c) GNPs/fBN_KH560, (d) GNPs15/BN, (e) GNPs15/fBN_KH550, (f) GNPs15/fBN_KH560	215
4.28	Lap shear strength of hybrid composites at different GNPs ratios	219
4.29	SEM images of fracture surfaces of hybrid composite (a) at GNPs5 ratio of 1.00, (b) GNPs5/BN at GNPs5 ratio of 0.75, (c) GNPs5/fBN_KH550 at GNPs5 ratio of 0.75 (d) GNPs5/fBN_KH560 at GNPs5 ratio of 0.75	224
4.30	SEM images of fracture surfaces of the hybrid composite at the ratio of 0.75 for (a) GNPs15/BN, (b) GNPs5/fBN_KH55, (c) GNPs5/fBN_KH560	227
4.31	Lap shear strength with the effect of moisture of hybrid composites at different GNPs ratios	230
4.32	SEM image of fracture surface at GNPs ratio of 0.75 (a) GNPs5/BN (b) GNPs5/fBN_KH550 (c) GNPs5/fBN_KH560 (d) GNPs15/BN (e) GNPs15/fBN_KH550 (f) GNPs15/fBN_KH560	234

LIST OF ABBREVIATIONS

0D	-	Zero-dimensional
1D	-	One-dimensional
2D	-	Two-dimensional
3D	-	Three-dimensional
AF	-	Adhesion failure
AEW	-	amine equivalent weight
APCF	-	Adhesion and cohesion failure with peel
ATR-FTIR	-	Attenuated total reflection –Fourier transform infrared spectroscopy
BN	-	Boron nitride
BS	-	Bath sonication
BeO	-	Berium oxide
BLT	-	Bond line thickness
C ₂ H ₅ OH	-	Ethanol
CB	-	Carbon black
CF	-	Carbon fibre
CF	-	Cohesive failure
Cu	-	Copper
CFS	-	Cohesive substrate failure
CNT	-	Carbon nanotube
C-O-C	-	Epoxide group
CPU	-	Central processing unit
CTE	-	Coefficient of thermal expansion
CVD	-	Chemical vapour deposition
DF	-	Delamination failure
DBC	-	Direct bound copper
DSC	-	Differential scanning calorimetry
EC	-	Electrical conductivity
ECA	-	Electrically conductive adhesives
EE	-	Energy-efficient
EEW	-	Epoxy equivalent weight
EV	-	Electric vehicles
fBN	-	Functionalised BN
FLG	-	Few layer graphene
GO	-	Graphene Oxide
GNPs	-	Graphene nanoplatelets
HDPE	-	High density polyethene
HEVs	-	Hybrid electrical vehicles
HSP	-	Hansen solubility parameter
ICs	-	Integrated circuits
IGBTs	-	insulated gate bipolar transistors
IHS	-	Integrated heat spreader
ITR	-	Interface thermal resistance
KH550	-	3-Aminopropyltriethoxysilane

KH560	-	3-Glycidoxypropyl-trimethoxysilane
LED	-	Light-emitting diode
LTJT	-	low temperature joining
MLG	-	Multi-layer graphene
MOSFETs	-	Metal-oxide-semiconductor field-effect transistors
MWCNT	-	Multi-wall carbon nanotube
NaOH	-	Sodium hydroxide
Ni	-	Nickel
-OH	-	Hydroxide functional groups
OLED	-	Omitted- light emitting diode
PDMS	-	Polydimethylsiloxane
Pb	-	Lead
PCM	-	Phase change materials
PCT	-	phase change temperature
PCTM	-	Planetary Centrifugal Thinky Mixer
RoHS	-	Restriction of hazardous substances directive
Sn	-	Tin
SF	-	substrate failure
SEM	-	Scanning electron microscopy
SET	-	Single-electron transistor
SiC	-	Silica carbide
SLJ	-	Single lap joint
SLG	-	Single layer graphene
SSA	-	Specific surface area
TBR	-	Thermal boundary resistance
TC	-	Thermal conductivity
TCA	-	Thermally conductive adhesives
TCE	-	Thermal conductivity enhancement
TCR	-	Thermal contact resistance
TIMs	-	Thermal interface materials
UH	-	Ultrasonic homogenizer
UTM	-	Universal tensile machine